Some characteristics of hydraulic jumps

N. S. LAKSHMANA RAO AND B. S. THANDAVESWARA*
Department of Civil Engineering, Indian Institute of Science, Bangalore 560 012, India

Received on July 7, 1977; Revised on October 25, 1977

Abstract

A semitheoretical analysis for the pre-entrained hydraulic jump shows 'the sequent depth ratio depends on the approaching flow air concentration'. Jump length may be defined arbitrarily. The energy loss is higher in the pre-entrained jump than in the normal jump and is a function of the Froude number.

Key words: Air entrainment, concentration, energy loss, sequent depth, length, hydraulic jump (normal, pre-entrained), stilling basin.

Introduction

Air entrainment and velocity distribution are two of the most important characteristics of a hydraulic jump. The other characteristics of the jump are sequent depth ratio, length of the jump and energy loss. Bélanger[1] was the first to derive a relationship for sequent depths by applying the momentum equation. Harleman[2] showed that neglecting of turbulent fluctuation balances the uniform velocity distribution. Bélanger's equation has been verified by many investigators experimentally and often a ratio lower than the one calculated by the equation has been recorded. Rajaratnam[3&4] corrected the momentum equation taking the bed shear force also into consideration. His equation gives a lower ratio of sequent depths for undeveloped flow and he points out that in the case of a jump with fully developed flow the sequent depth may be higher than that predicted by his equation. Leutheusser and Vishwanathan[5] observed that for reasons which are not yet clear, jumps with undeveloped upstream flows show larger sequent depth ratios and smaller lengths than jumps with fully developed flows. Further, it is to be noted that whenever one compares the sequent depths it is essential to be clear about the definition adopted for the length of the jump. The length of the jump is also important in designing stilling basins. The beginning of the jump or the toe of the jump may easily be fixed as the mean position of the oscillation at the abrupt rise of the water surface. But there has not been any general accord as to the end of the jump and has become a controversial matter for the past few decades. According to Rouse *et al*[6] the jump length is arbitrary because the jump never ends but only approaches asymptotically a state of depth, velocity and turbulent

* Department of Civil Engineering, Indian Institute of Technology, Madras 600 036, India.

equilibrium. Several investigators have proposed varying definitions of the length of the jump[7, 8] based on the following considerations:

(i) Up to the end of the roller[7 & 8], (ii) based on 2% mean air concentration[3], (iii) based on depth of flow[3, 8 & 9], (iv) up to a distance at which the bed velocity is a certain percentage of the approach flow[10], (v) uniform velocity distribution criterion[5] and (vi) based on the force exerted by the flow at the end of the jump on a cylindrical body[8 & 11].

Each one of the definitions is justifiable in its own way from the point of view of field applications depending on specific needs. The end of the roller may be chosen for stilling basic design provided the downstream is composed of hard rock. On the other hand, if the downstream consists of movable materials such as loose sand or pebbles, then the criterion of a certain percentage of approach velocity on the bed appears more reasonable. While designing the stilling basin as a roof of a power house, where random stresses have to be accounted for, the criterion of pressure fluctuation,[9] and when the weight component of two phase flow is to be considered, Rajaratnam's suggestion suits best. From the analytical point of view the end portion of the jump is that where all the effects due to the jump inclusive of air entrainment and turbulence are completely absent. However, recently (1976) Mehrotra[12] analysed the length of the jump on the assumption that the turbulent roller comprises energy containing eddies which feed upon the flow outside the roller and decay follows the well-known laws of decay for such eddies. The assumption of isotropic characteristics of turbulence in itself is indeed open for criticism.

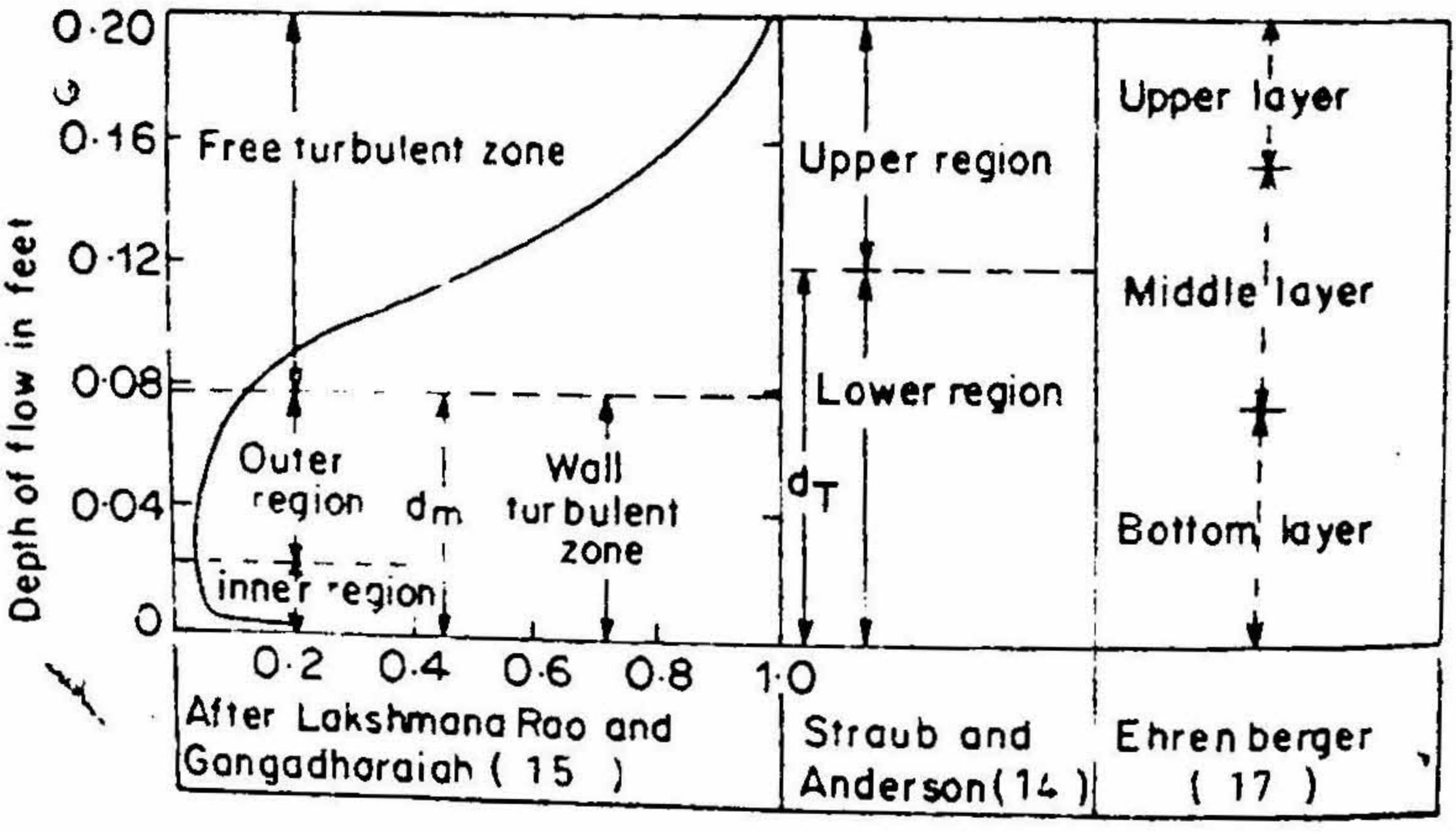

FIG. 1. Classification of aerated flow regions.

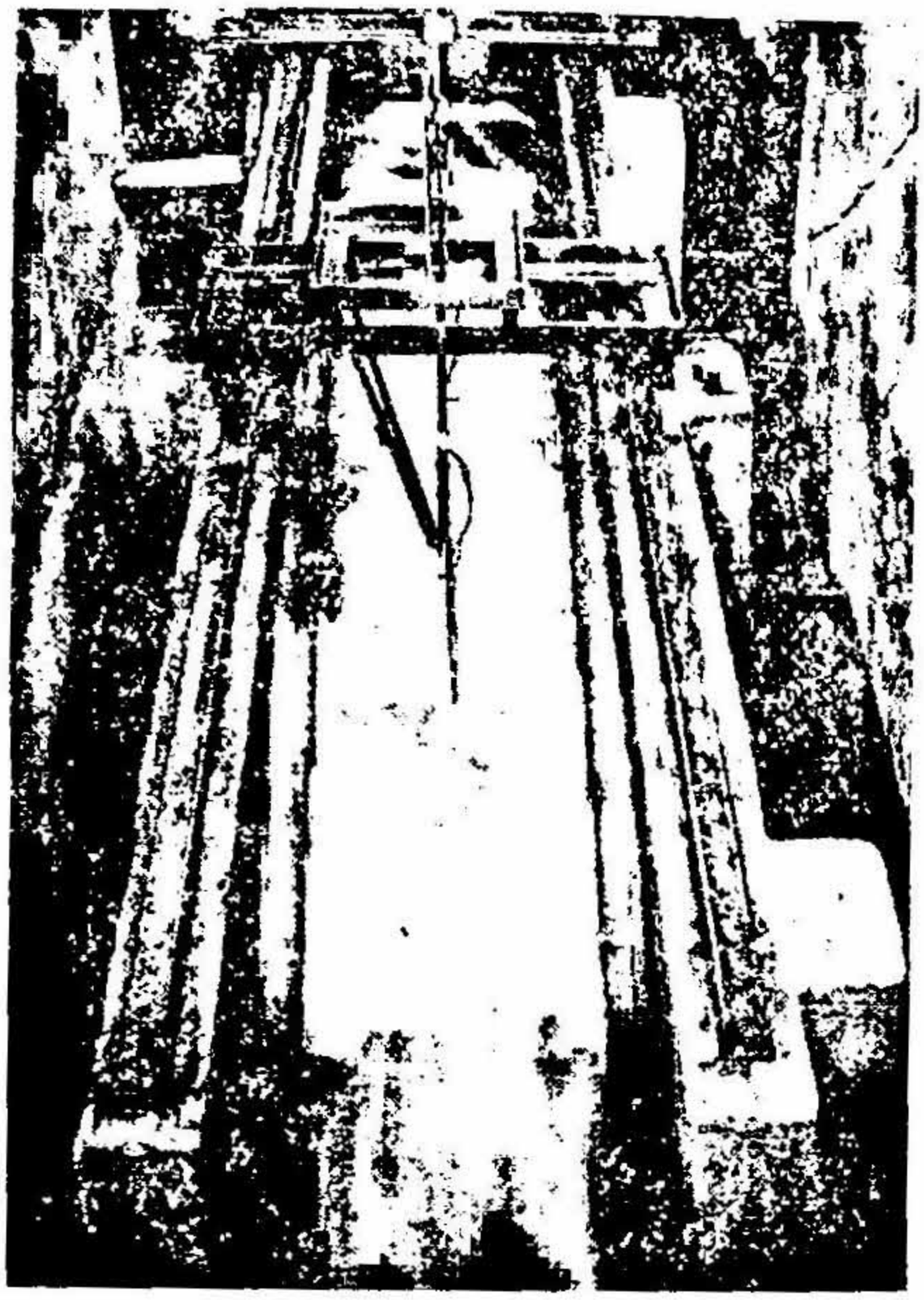

FIG. 2. View of the Pre-entrained Hydraulic Jump (PHJ).

FIG. 3. Plan view of the Normal Hydraulic Jump (NHJ).

The energy loss due to the jump has also been investigated by many investigators.[3 & 7] However, all these investigations were carried out on a 'Normal hydraulic jump (NHJ)' There seems to be hardly any information about such characteristics in the case of 'Pre-entrained hydraulic jump (PHJ)'. The jump, created with an approach flow with aerated conditions such as near the toe of the spillways, is called the 'pre-entrained hydraulic jump (PHJ)'. In the present paper results of a comparative study of the NHJ and the PHJ are presented.[13]

Definitions: Some definitions for aerated flow as proposed by several investigators[14–16] for terms such as air concentration (C); mean air concentration, $\bar{C}$; transitional mean concentration, $\bar{C}_T$; mean depth $\bar{d}$; transitional depth, d_T; upper limit of the flow, d_s; and mixing width b have been used. Fig. 1 shows the classifications of the aerated flow section. Straub and Anderson[14] divided the flow into an upper region and a lower region whereas Lakshmana Rao and Gangadharaiah[15] classified this into the free turbulent zone and the wall turbulent zone. Ehrenberger[17] divided the flow into three regions which has also been shown in Fig. 1.

Experimental set ups

Two experimental set ups were used in this investigation. A tilting flume along with a horizontal masonry channel at its end was used for studying the characteristics of the

PHJ. Another set up consisting of a 10·35 m long, horizontal smooth wide channel with a bellmouth transition was used. The general views of the PHJ and the NHJ are shown in Figs. 2 and 3 respectively. The electrical probe[13] developed at the Indian Institute of Science was used for measuring the air concentration. The velocity was measured using a pitot tube. The mean position of the toe of the jump is taken as the origin and distance x, downstream is reckoned positive. The initial depths y_1 and y_{1*} are used for normalizing the parameters for the NHJ and the PHJ respectively. A summary of the experimental details is shown in Table I.

Results and discussions

Momentum Equation: The flow in this investigation was not fully developed. Fig. 4 shows that the sequent depth ratio for the NHJ is higher than that predicted by Bélanger's momentum equation. In this case, only one run gave a value equal to that of the Bélanger's equation. This difference is due to the basic assumptions made in deriving the momentum equation such as neglecting the shear and air entrainment, and variation of turbulence level.

In the case of the PHJ, there is little information available regarding the effect of air entrainment on sequent depth. Earlier investigators[3] presented empirical equations

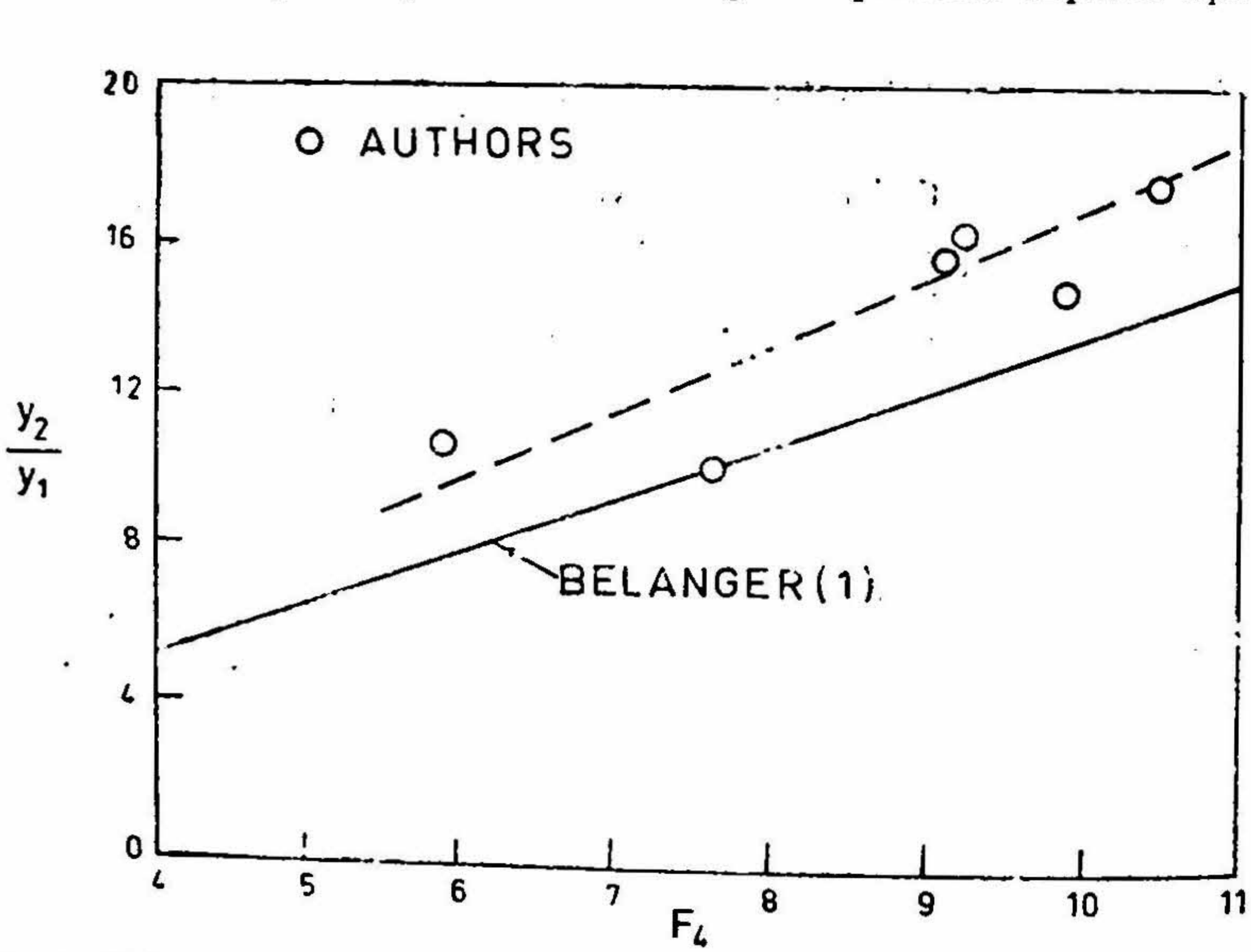

FIG. 4. Variation of sequent depth ratio with Froude number (NHJ).

Table I

Experimental Details

Pre-entrained Hydraulic Jump

	Series B			Series E			
Run No.	B4	B0	B2	B3	E0	E2	E3
Discharge 1/sec.	28·32	42·48	56·41	71·22	28·32	56·41	71·22
Re_1	65680	98520	130840	165190	66800	133070	168000
F_1	6·03	5·10	4·23	5·11	5·49	5·89	5·19
y_{1*} in cm.	2·38	3 23	4·43	4·56	2·35	3·55	4·51

Normal Hydraulic Jump

Run No.	R1	R2	R3	R4	R5	R6
Discharge 1/sec.	18·41	21·24	25·49	29·79	34·21	37·10
F_4	5·92	7·64	9·14	9·22	10·47	9·88
Re_1	32340	37310	44780	52340	59510	65170
y_1	1·22	1·31	1·07	1·16	1·22	1·52

Note : 2 *cfs* = 18·32 *l*/sec ; $y_{1*} = d_1 = \int_0^{d_m} (1 - c)\, dy$;

y_1 = depth measured up to free surface (NHJ).

which yielded contradictory results. Rajaratnam[3] attempted to present a rational theory for the PHJ. In this section an attempt is made to include the density variation due to air entrainment in aerated flow, along with the assumption of similarity of

velocity distribution for the PHJ. The schematic diagram of the PHJ is shown in Fig. 5. The following assumptions are made in the analysis, namely, (i) the bed slope is zero and the approaching flow is uniformly aerated, (ii) no air is present at the end of the jump, (iii) hydrostatic pressure distribution exists at the toe of the jump, (iv) the turbulent

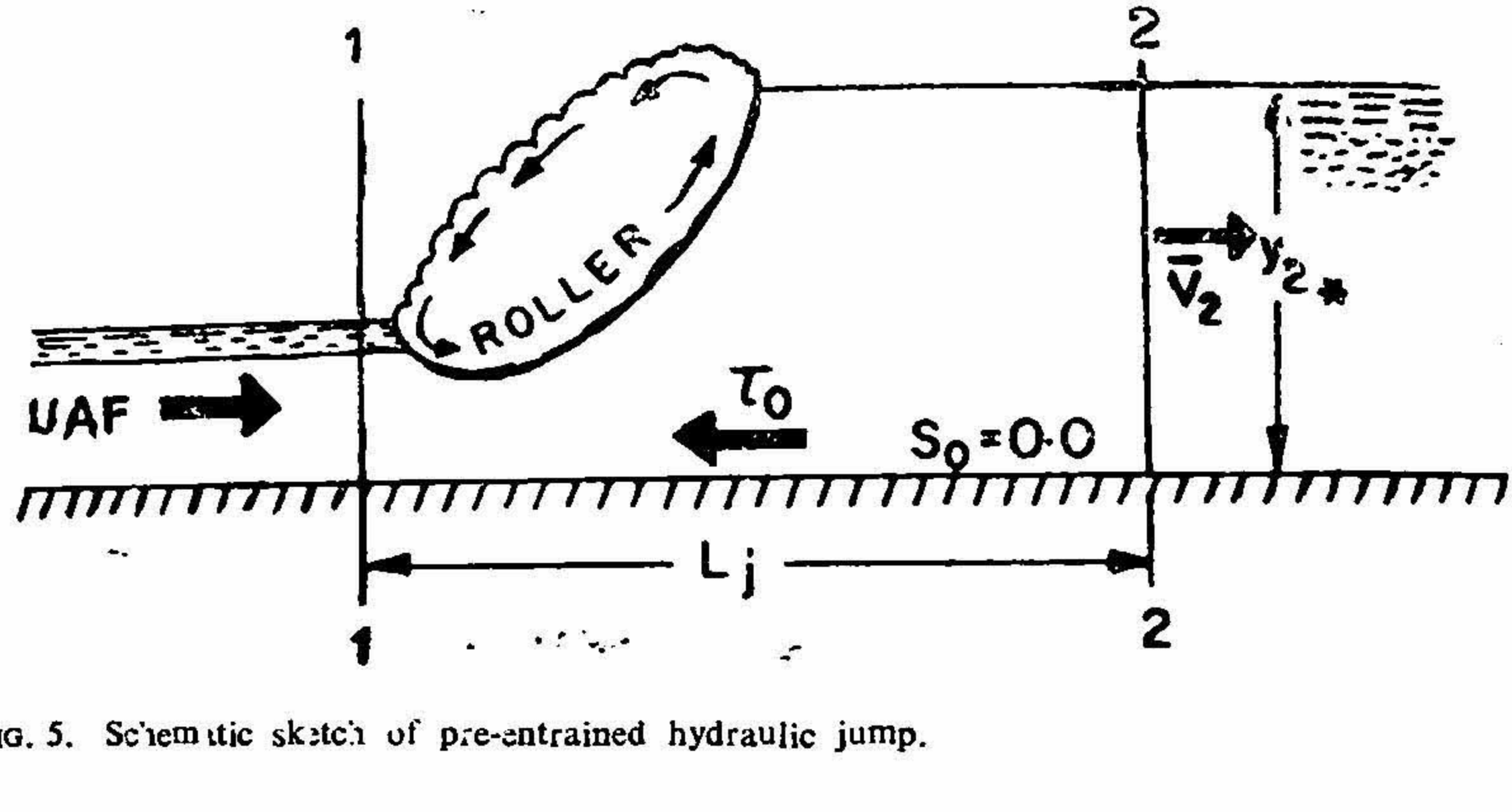

FIG. 5. Schematic sketch of pre-entrained hydraulic jump.

contribution to the momentum and the effect of variation of velocity with depth along the jump is neglected as they have a tendency to balance each other and are small[2] and (v) the velocity and the concentration distributions of the approach flow section are as shown in Fig. 6.

Computation of momentum is carried out as follows:

(*a*) Referring to Figs. 5 and 6, the mean velocity at section 1–1 for the wall region, the intermediate region ($d_T - \delta$), and the upper region may be written as

$$\left.\begin{aligned} \bar{V}'_1 &= \frac{1}{\delta}\int_0^{\delta} v\,dy \\ \bar{V}'_2 &= \frac{1}{d_T - \delta}\int_{\delta}^{d_T} v\,dy \end{aligned}\right\} \qquad (1)$$

and

$$\bar{V}_3 = \frac{1}{d_{u_1} - d_T}\int_{d_T}^{d_{u_1}} v\,dy$$

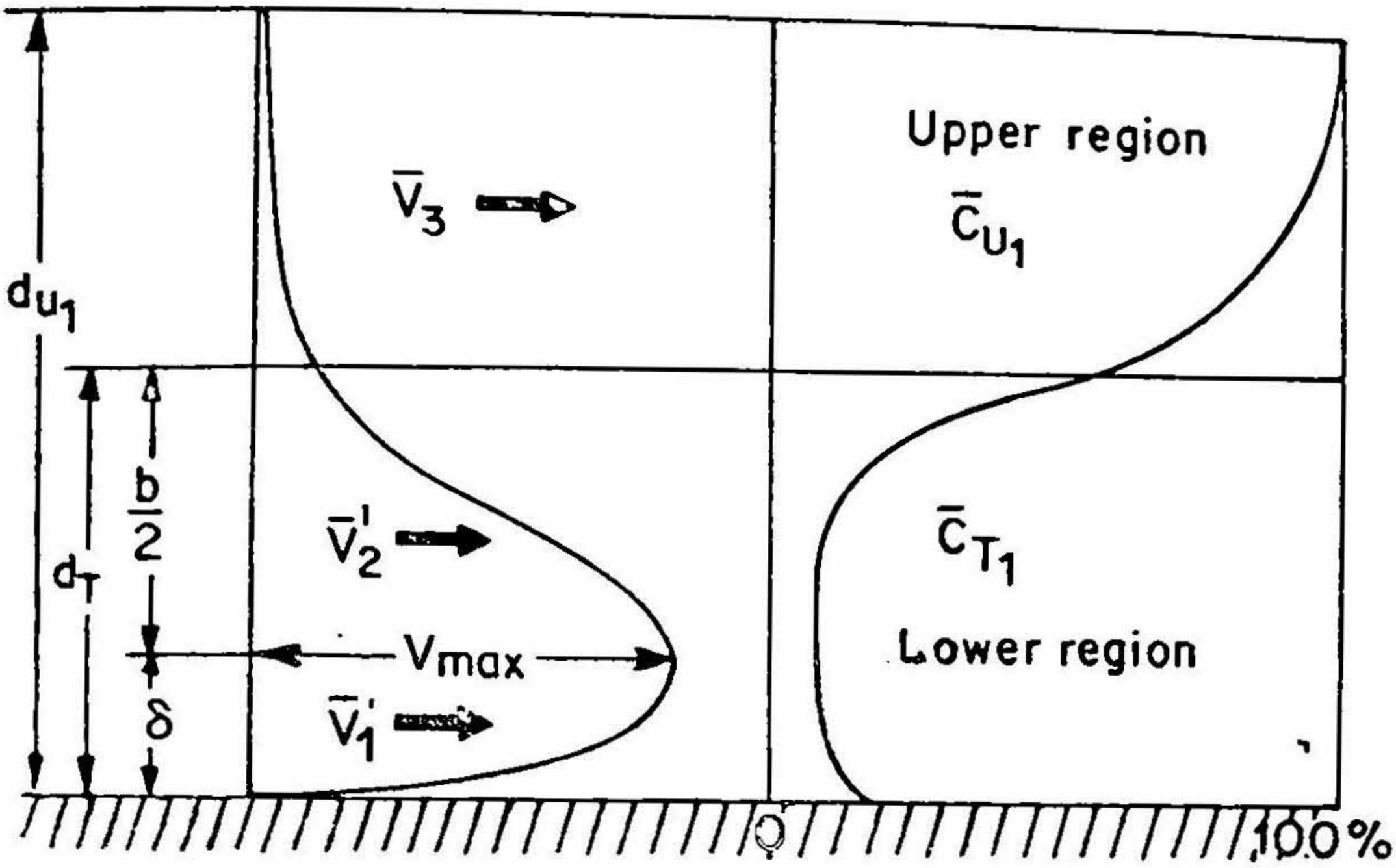

FIG. 6. Velocity and air concentration distributions at section 1–1.

in which δ is the wall turbulent thickness. d_T is the transitional depth and d_{u_1} is the upper limit of the flow. The mean air concentration in the lower and upper regions may respectively be written as

$$\bar{C}_{T_1} = \frac{1}{d_T} \int_0^{dT} C\, dy \tag{2}$$

and

$$\bar{C}_{U_1} = \frac{1}{d_{u_1} - d_T} \int_{d_T}^{d_{u_1}} C\, dy\,. \tag{3}$$

Assuming unit width of the flow, the momentum at section 1–1, after correcting for the density of aerated flow (using the equation of Lakshmana Rao *et al*[16]), may be written as

$$\begin{aligned} \delta\,(1 - 1{\cdot}1\,\bar{C}_{T_1})\frac{\gamma}{g}\,\bar{V}'^{2}_{1} + (1 - 1{\cdot}1\,\bar{C}_{T_1})\frac{\gamma}{g}\,\bar{V}'^{2}_{2}\frac{b}{2} \\ + \left[(d_{u_1} - d_T)\,(1 - 1{\cdot}1\,\bar{C}_{U_1})\frac{\gamma}{g}\,\bar{V}_3^{2}\right] \end{aligned} \tag{4}$$

in which γ is the specific weight of water and $b/2$ is the half mixing width,

The momentum at section 2–2 may be written as

$$\frac{\beta_1 \bar{V}_2^2 y_{2*} \gamma}{g} \tag{5}$$

in which β_1 is the momentum coefficient for nonuniform velocity distribution and $\bar{V}_2$ is the mean velocity at section 2–2. Now, the equations for different forces may be written as follows:

(*a*) Taking the density variation[16] for the lower and upper regions, the pressure force at section 1–1 is equal to

$$\gamma d_T \left[(1\text{–}1\cdot1\ \bar{C}_{U_1}) \left(\frac{d_{u_1}}{2d_T} - \frac{1}{2} \right) \{ d_{u_1} + d_T \} + 2\,(1\text{–}1\cdot1\ \bar{C}_T)\, d_T \right] \tag{6}$$

and at section 2–2 is equal to

$$\frac{\gamma y_{2*}^2}{2} \tag{7}$$

(*b*) *Shear force* : The boundary shear stress, τ_0, may be taken as[4]

$$\tau_0 = c_f \frac{\rho_{aw}}{2} V_{max}^2 \tag{8}$$

in which c_f, the local skin friction coefficient, may be taken as

$$c_f = \frac{0\cdot0424}{\left(\frac{V_{max}\,\delta}{\nu} \right)^{0\cdot25}} \tag{9}$$

in which V_{max} is the maximum velocity at the cross section, ρ_{aw} is the mass density of air water mixture, and ν is the kinematic viscosity.

Using eqs. (8) and (9) and integrating the shear stress over the length of the jump (L_j) yields

$$P_f = K_1 \gamma \int_0^{L_j} V_{max}^{1.75}\, \delta^{-0.25}\, dx \tag{10}$$

in which

$$K_1 = \frac{0\cdot0424\ \nu^{0.25}}{2g}.$$

Applying the principle that the rate of change of momentum equals the external force to the free body diagram (Fig. 6) of the PHJ and using eq. (1) to (10), the momentum equation may be written as

$$\phi^2 + 2\beta_1 F_8^2 \phi - \frac{\delta}{d_{u_1}} F_5^2 A_2 - \frac{b}{d_{u_1}} F_6^2 A_2 - 2d_T \left(\frac{d_{u_1}}{d_T} - 1\right) F_7^2 A_1$$

$$- \left(\frac{d_T}{d_{u_1}}\right)^2 \left\{\left(\frac{d_{u_1}}{d_T}\right)^2 - 1\right\} A_1 - 4\left(\frac{d_T}{d_{u_1}}\right)^2 A_2 + \frac{P_f}{d_{u_1}^2} \frac{2}{\gamma} = 0 \qquad (11)$$

in which

$$A_1 = (1 - 1 \cdot 1\, \bar{C}_{U_1}), \quad A_2 = (1 - 1 \cdot 1\, \bar{C}_{T_1}), \quad \phi = \frac{y_{2*}}{d_{u_1}},$$

$$F_5^2 = \frac{\bar{V'}_1^2}{g d_{u_1}}, \quad F_6^2 = \frac{\bar{V'}_2^2}{g d_{u_1}}, \quad F_7^2 = \frac{\bar{V}_3^2}{g d_{u_1}}, \quad F_8^2 = \frac{\bar{V}_2^2}{g d_{u_1}}.$$

Using the results of Sigalla[13] for the wall jet, the following values may be assumed, namely

$$\left.\begin{aligned} & d_{u_1} = 2 \cdot 25\, d_T, \quad \delta = 0 \cdot 16\, d_T, \quad b = 0 \cdot 7466\, d_{u_1} \\ \text{and} \quad & \\ & \delta = \cdot 07111\, d_{u_1}. \end{aligned}\right\} \qquad (12)$$

Substituting the values from eq. (12) in eq. (11), it may be rewritten as

$$\phi^2 + 2\beta_1 F_8^2 \phi - A_2 \{\cdot 07111\, F_5^2 + 0 \cdot 7466\, F_6^2 + 0 \cdot 790\}$$
$$- A_1 \{2 \cdot 50\, d_T F_7^2 + 0 \cdot 8024\} + p'_f = 0 \qquad (13)$$

in which

$$p'_f = \frac{2K_1}{d_{u_1}^2} \int_0^{L_f} V_{\max}^{1.75}\, \delta^{-0.25}\, dx.$$

It may be seen from eq. (13) that the sequent depth ratio reduces due to air entrainment and that the major contributing factor is the lower region. This is in agreement with the theoretical analysis of Rajaratnam.[3]

The variation of the sequent depth ratio with Froude number for the PHJ is shown in Fig. 7. It shows a higher value than that given by Bélanger's equation, confirming the earlier observations with respect to the NHJ (Fig. 4). The extra sequent depth recorded is around 29·5%. The PHJ gives a higher sequent depth ratio than the NHJ. However, eq. (13) has to be verified experimentally which has not been made in this study due to difficulties in controlling the mean concentration of the approach flow and to vary it systematically.

Roller depth, y_{rj} : The roller depth was taken at the section at which the zero isovel meets the free surface. The relationships between y_{rj}/y_2 and the initial Froude number for the NHJ and the PHJ are shown in Figs. 8 and 9. Two empirical relations, namely,

$$\frac{y_{rj}}{y_2} = 0{\cdot}623 + 0{\cdot}05156\, F_1 \tag{14}$$

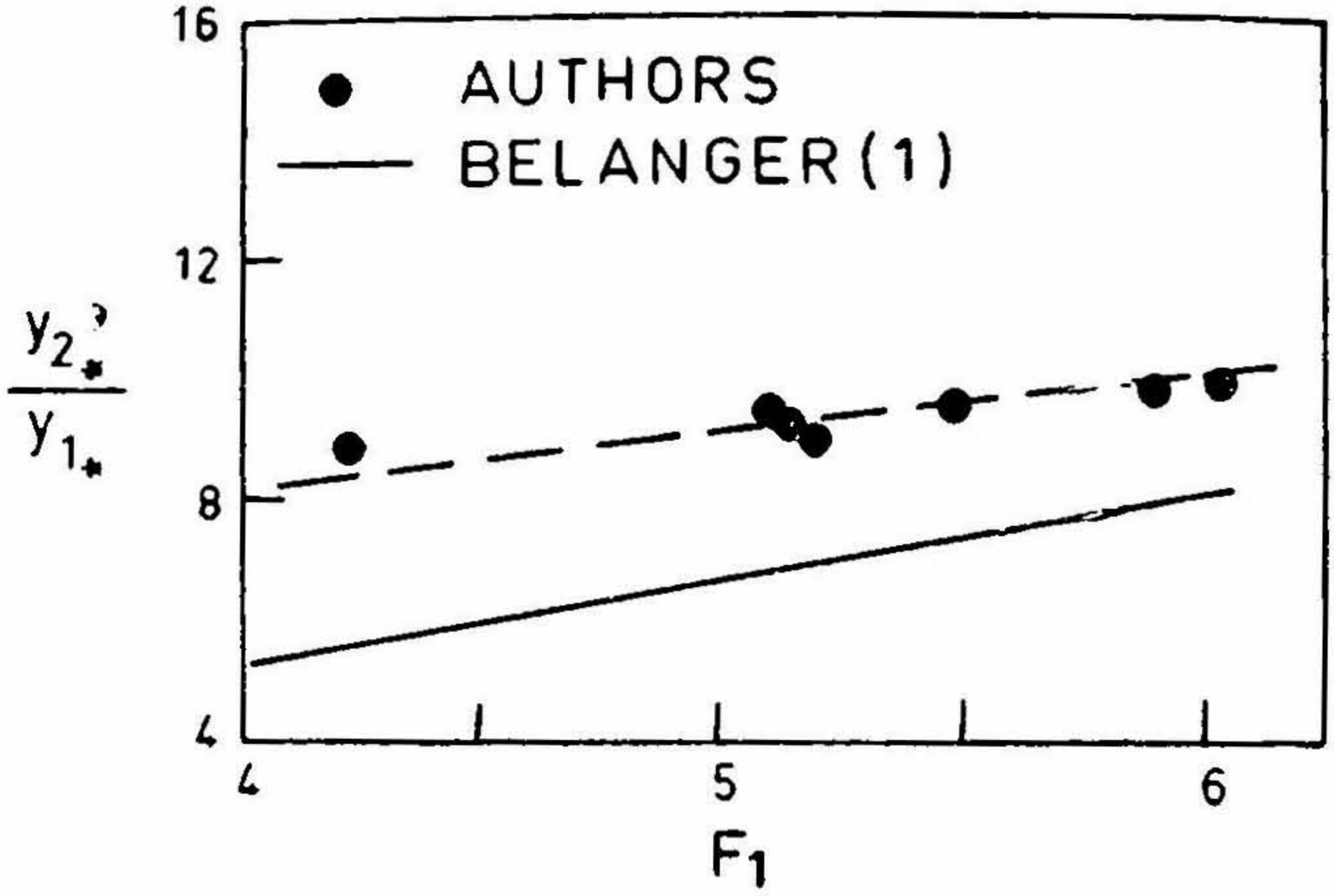

FIG. 7. Variation of sequent depth ratio with Froude number (PHJ).

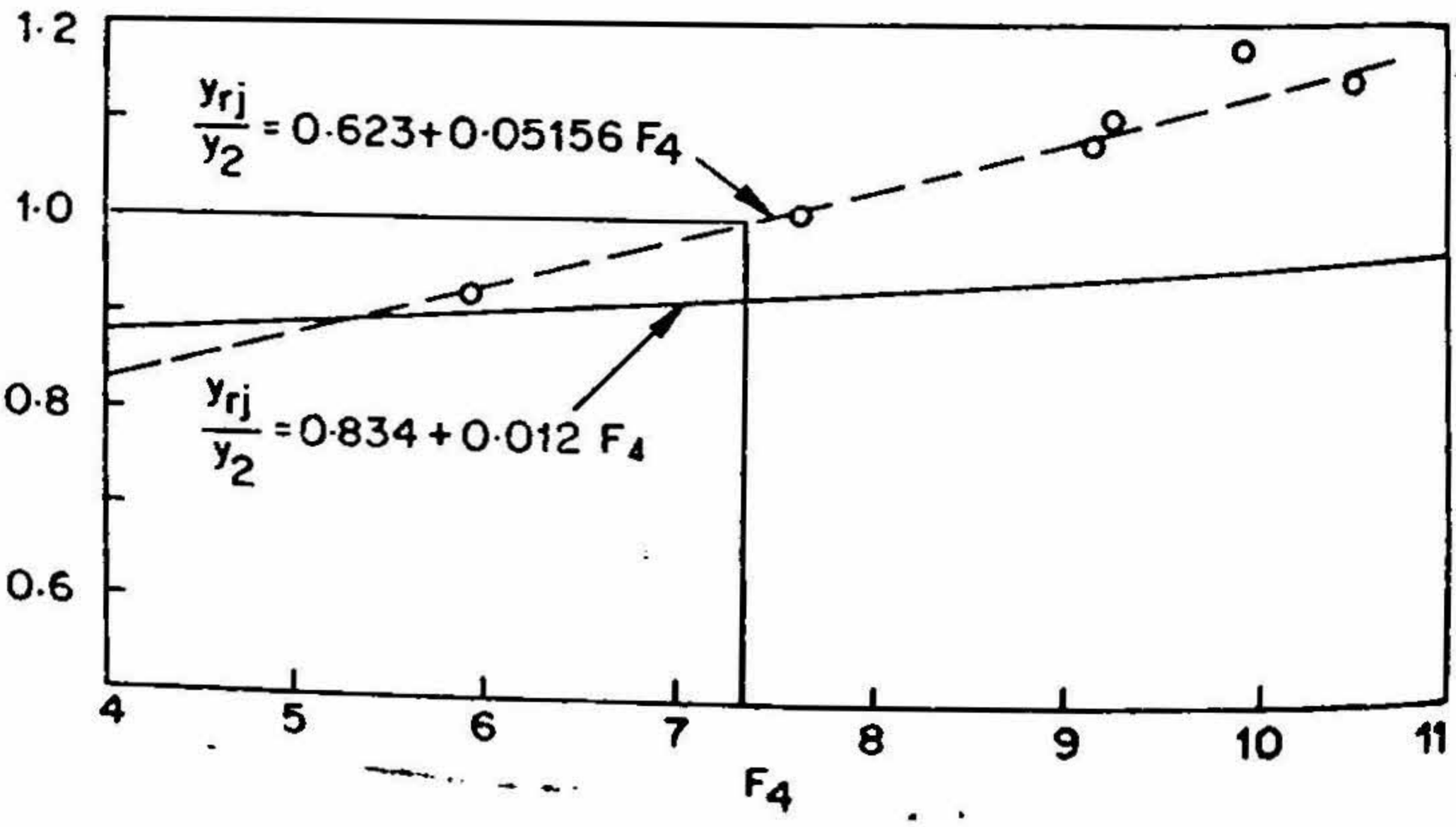

FIG. 8. Relationship between y_{rj}/y_2 and F_4 (NHJ).

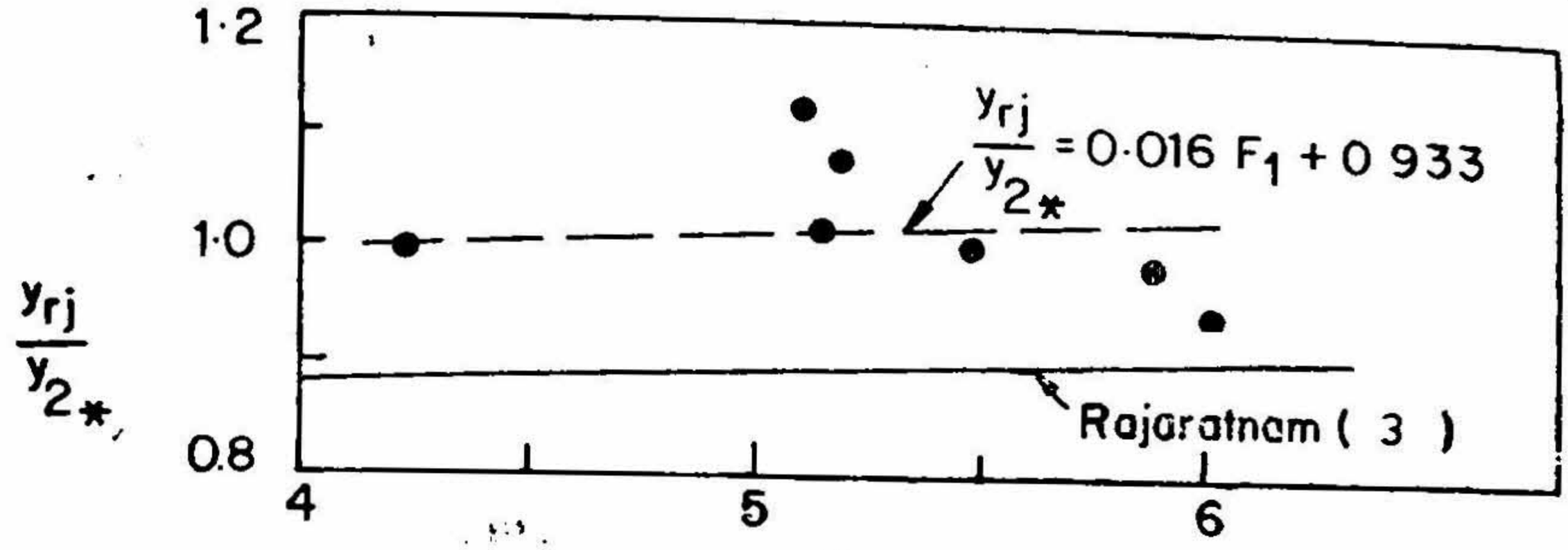

FIG. 9. Relationship between y_{rj}/y_{2*} and F_1 (PHJ).

and

$$\frac{y_{rj}}{y_{2*}} = 0{\cdot}933 + 0{\cdot}016\, F_1 \tag{15}$$

may be fitted to the experimental data.

Length of the jump : Several lengths based on the experimental observations may be defined as follows:

(i) *Length of intake zone, L_I, and length of releasing zone, L_R*: These lengths are defined based on the distribution of mean concentration along the jump.[3] The distance from the toe to the point at which the mean air concentration reaches a maximum value is taken as the 'length of the intake zone' (L_I) and beyond this point to the section at which 2% mean air concentration exists is taken as the 'length of the releasing zone' (L_R).

(ii) *Length of the roller, L_{rj}* : The horizontal distance between the toe of the jump to that section at which the zero isovel emerges to the free surface is taken as the length of the roller.

(iii) *Length of the jump, L_{vj}*: This is based on the veloctiy distribution along the jump. After a certain distance, the flow attains uniform velocity distribution conditions, which fixes the length of the jump from the toe.

(iv) *Rajaratnam's criterion, L_{ej}*: is the sum of the air intake (L_I) and the air release zone (L_R). This distance is arbitrary in the sense that one may choose the distance at which either 5% or 1% mean concentration or any other value exists.

(v) *Length of kink, L_{ckj}* : This definition is based on the air concentration distribution. In the beginning of the jump the air concentration profiles exhibit kinks and values may vary very rapidly in this region. The distance between the toe and the point of disappearance of these kinks is taken as the kink length, L_{ckj} from the concentration distribution plots.[13, 19]

Figs. 10 and 11 show the normalized length characteristics for both the NHJ and the PHJ respectively. However, the data from Rajaratnam's[20] results are also utilised

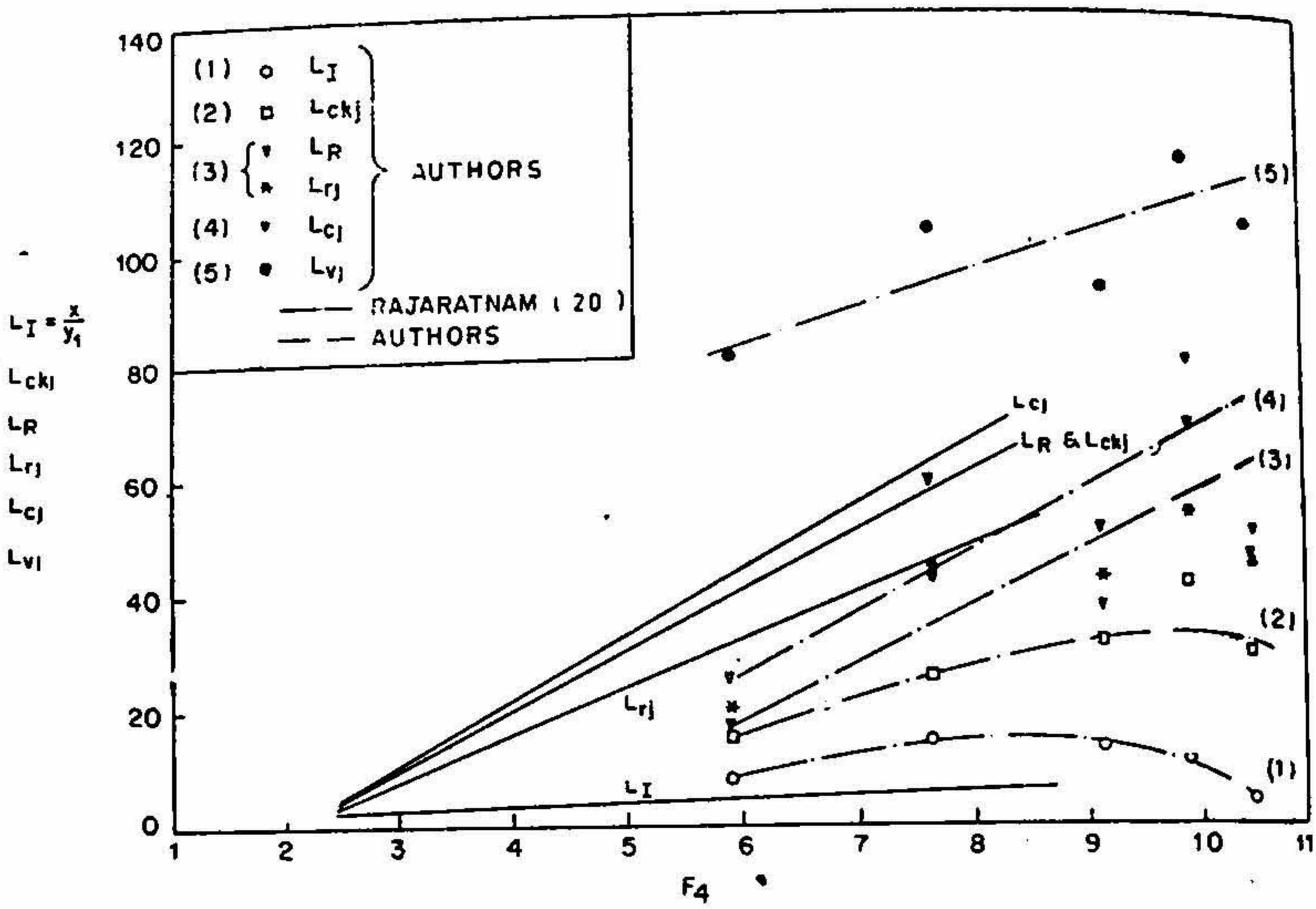

FIG. 10. Length characteristics of the jump (NHJ).

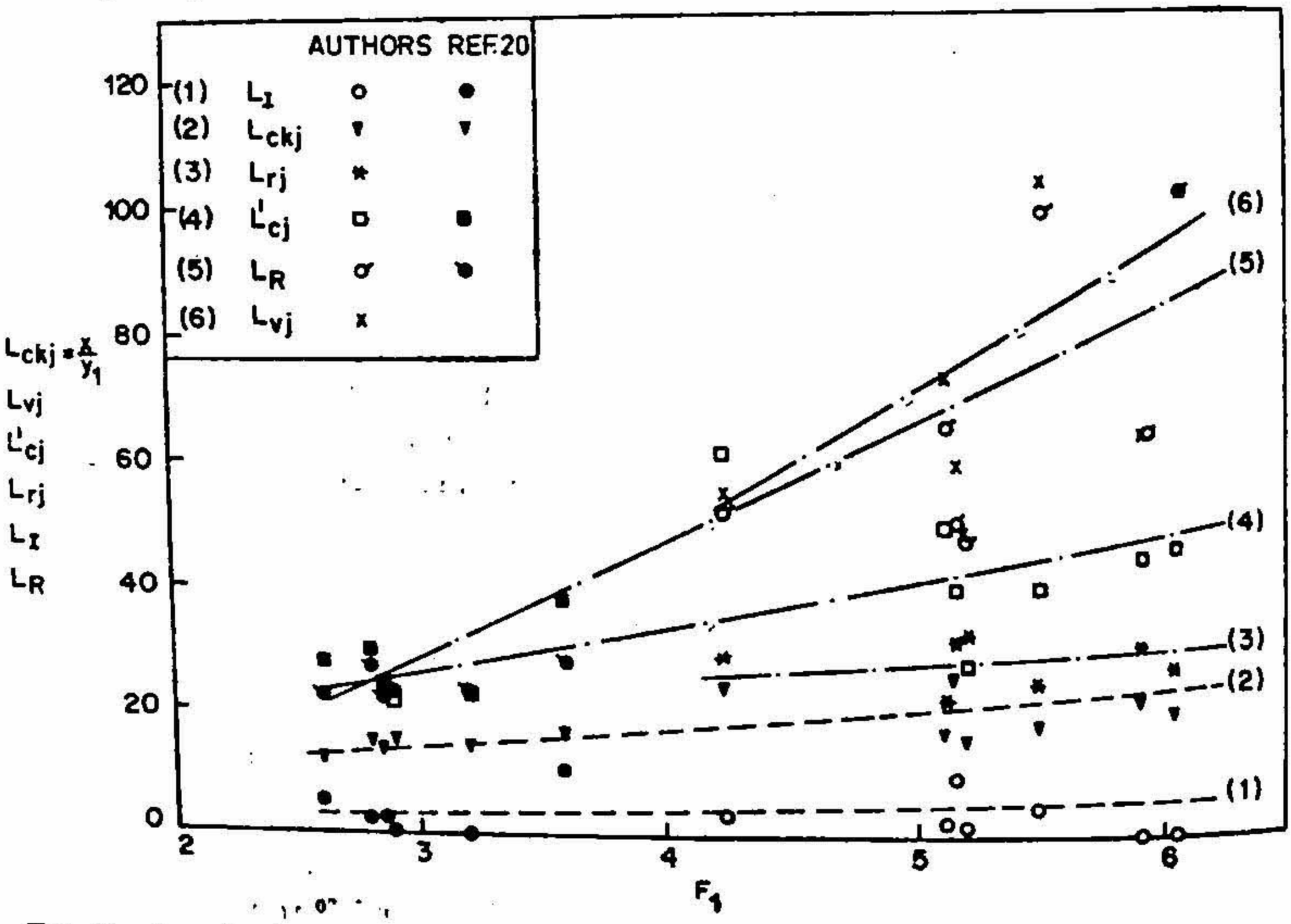

FIG. 11. Length characteristics of the jump (PHJ).

and general trends are shown in Fig. 10. It may be seen from the figures that $L_{oj} > L_{ej} > L'_{oj} > L_{rj} > L_{ckj} > L_j$. These lengths show an increasing tendency with Froude number. The L_R is of the same order of magnitude as L_{ckj}. In the case of the PHJ, L'_{oj} is taken as the distance at which 8% mean concentration exists, as the length of the flume was small and the measurements could not be taken till $\bar{C}$ reaches 2%. The releasing zone in the PHJ is greater than in the NHJ.

Variation of relative distances with Froude number is shown in Figs. 12, 13 and 14. The relative intake zone length reduces as the Froude number increases and varies

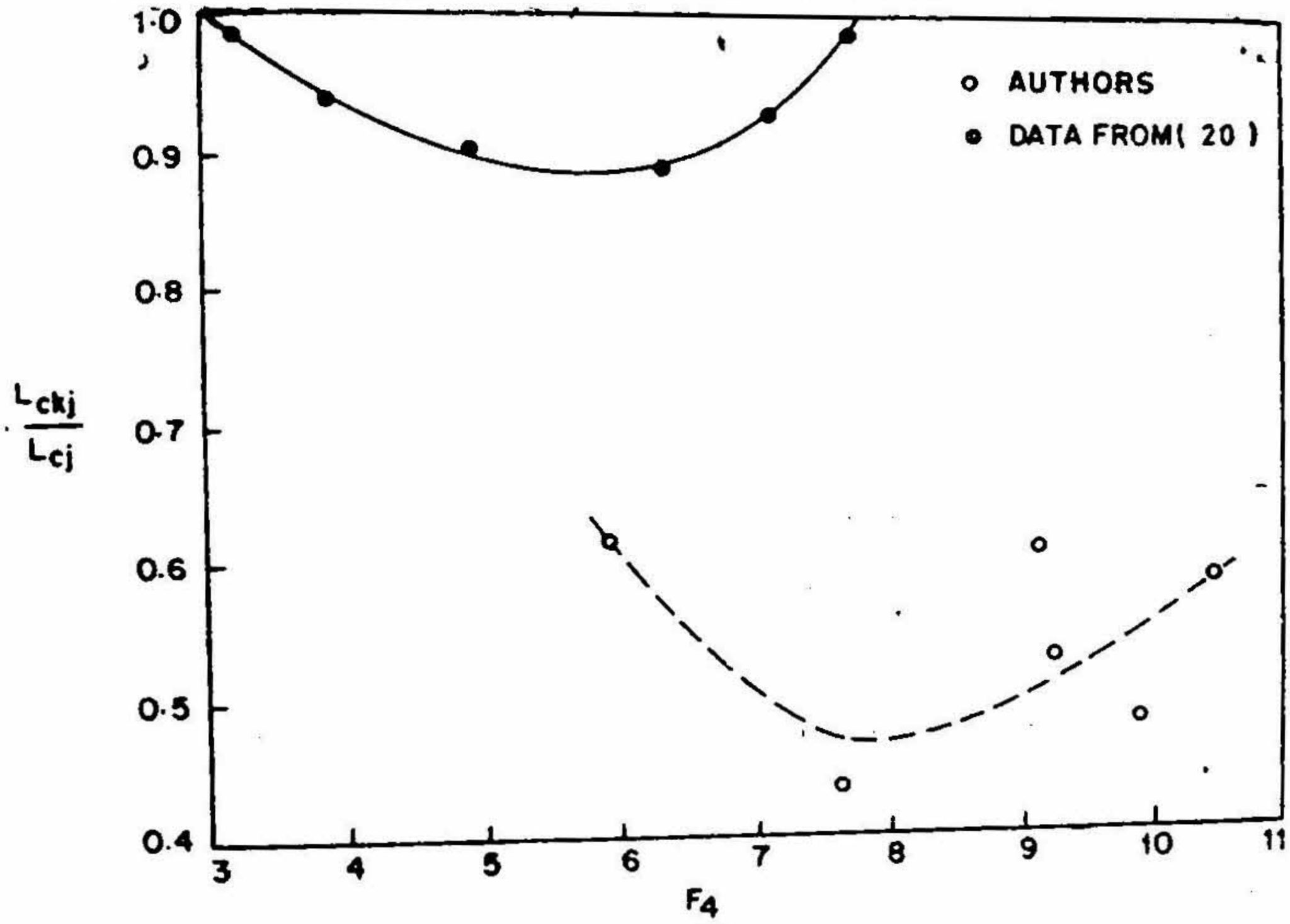

FIG. 12 *a*

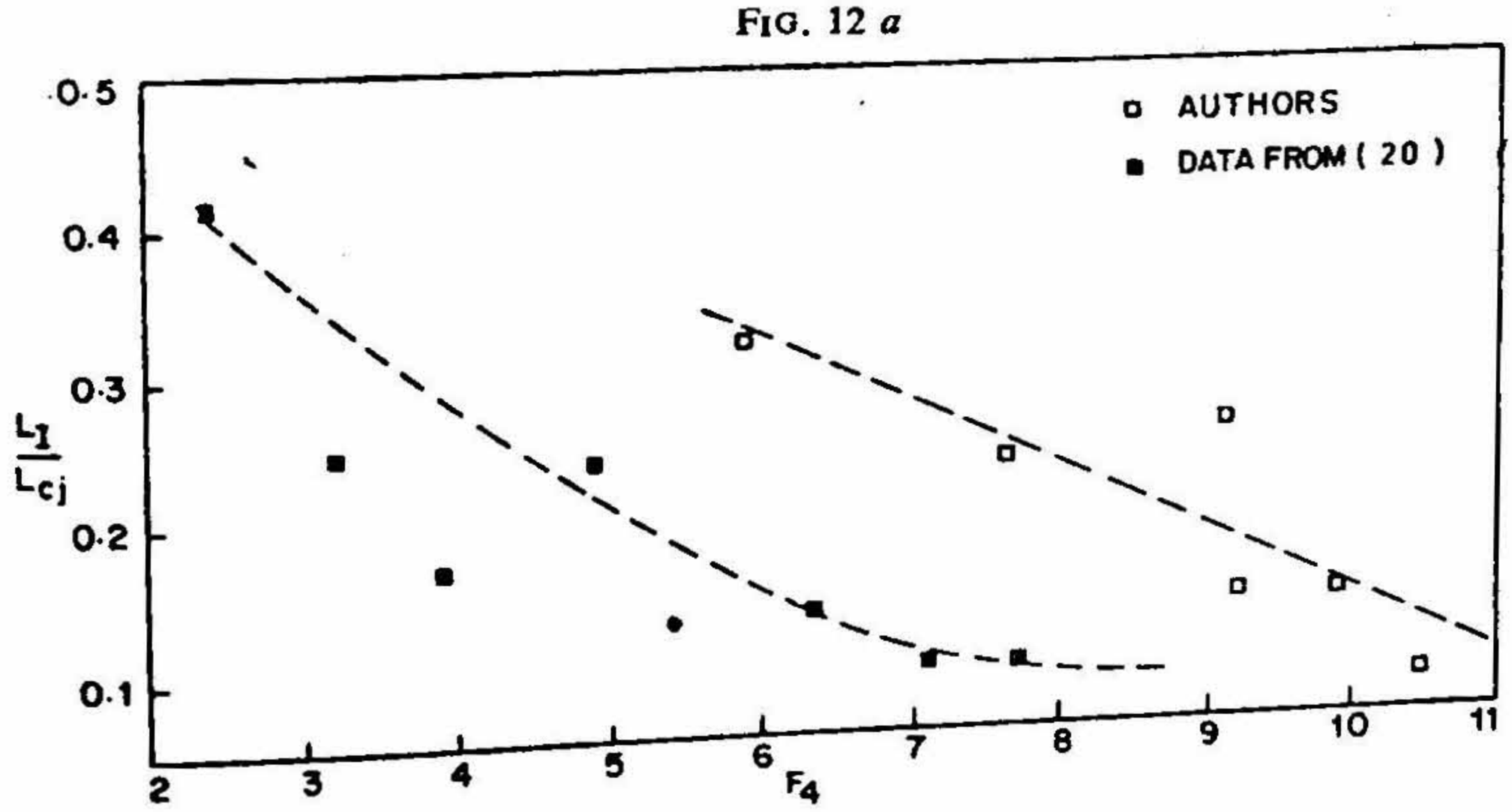

FIG. 12 *b*

FIG. **12 *a* & *b*. Variation of relative distances with Froude number (NHJ).**

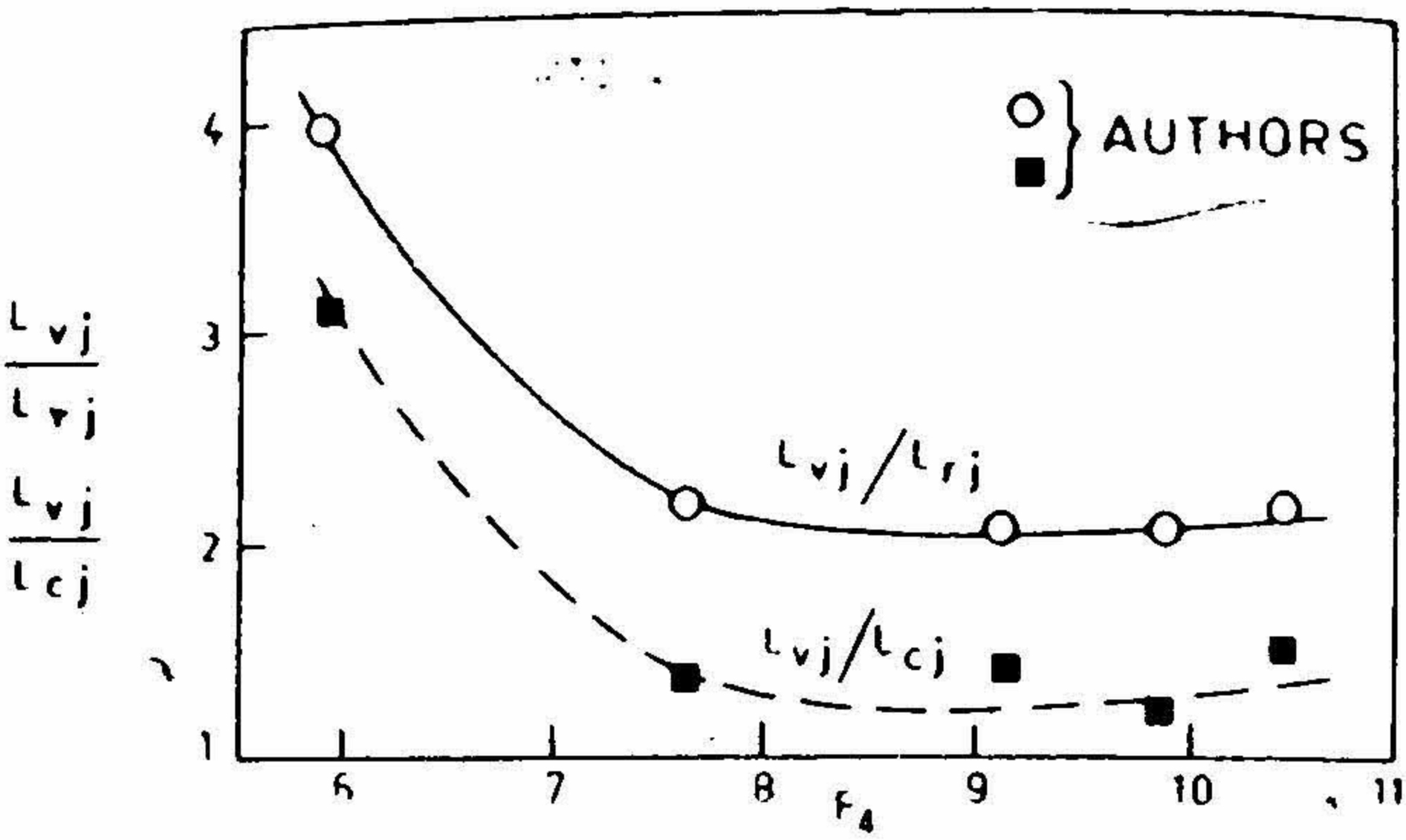

FIG. 13. Variation of relative distances with Froude number (NHJ).

from 0·42 to 0·05 in a Froude number range of 2 to 11·0. But L_{ckj}/L_{cj} gradually decreases as the Froude number increases (Fig. 12), reaches a minimum value and shows an increasing tendency further with Froude number. The releasing zone shows an opposite trend to the variation of the intake zone. The roller length is found to increase with the Froude number. It may be observed from Fig. 13 that the relative lengths decrease sharply in the lower range of Froude numbers and remain practically constant in the upper ranges. The ratio of the length of the jump, L_{rj}, to that of the roller L_{rj} is around 2·2 and L_{vj}/L_{cj} is around 1·5 beyond a Froude number value of about 7·6.

In the case of the PHJ no definite conclusions could be drawn as the experimental Froude number range was very small. It was observed that $L_{rj} > L_{ckj} > L_I$. While L_{vj}/L_{rj} does not exhibit any trend, the other two namely, L_{cj}/L'_{cj} and L_{vj}/L_R exhibit linear variations (Fig. 14).

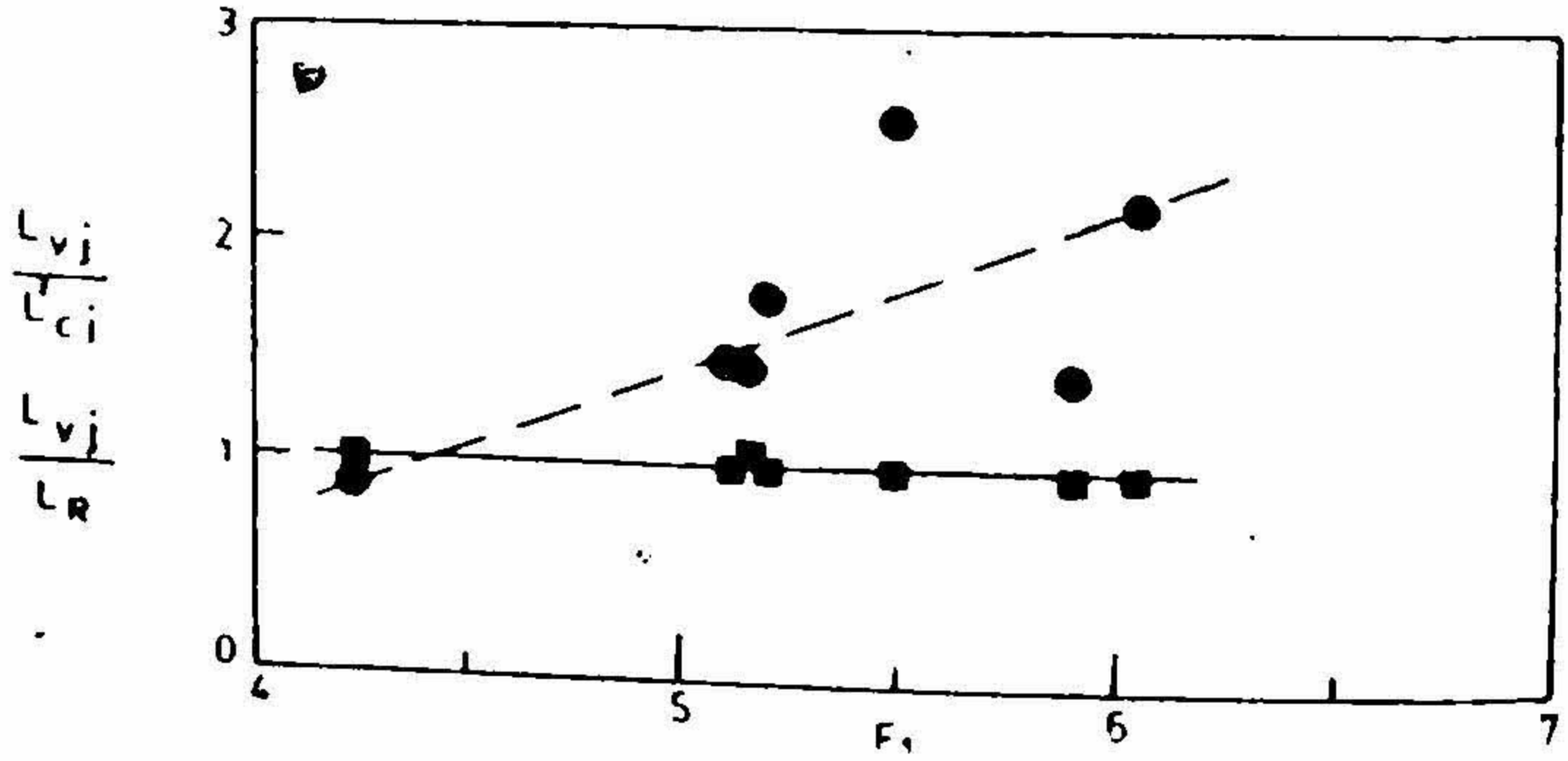

FIG. 14. Variation of relative distances with Froude number (PHJ).

In the case of the PHJ, unlike in the NHJ, the wall concentration exists even before the toe of the jump. After the jump, this wall concentration becomes zero at a certain distance from the toe. This distance L_{cwo} shows an increasing tendency with Froude number (Fig. 15).

Relative energy loss: Based on the specific energy concept[7] the energy loss, E_L, for the jump was computed. Fig. 16 shows the relative energy loss E_L/E_1 for both the NHJ and the PHJ. The PHJ is found to have more relative energy loss than the NHJ for a given Froude number and increases with it. As the Froude number increases the transitional mean air concentration, $\bar{C}_T$, increases.[14] The theoretical prediction of Rajaratnam shows that the relative energy loss is a function of transitional mean air concentration of the approach flow. Hence the effect of increase in concentration is to increase energy loss.

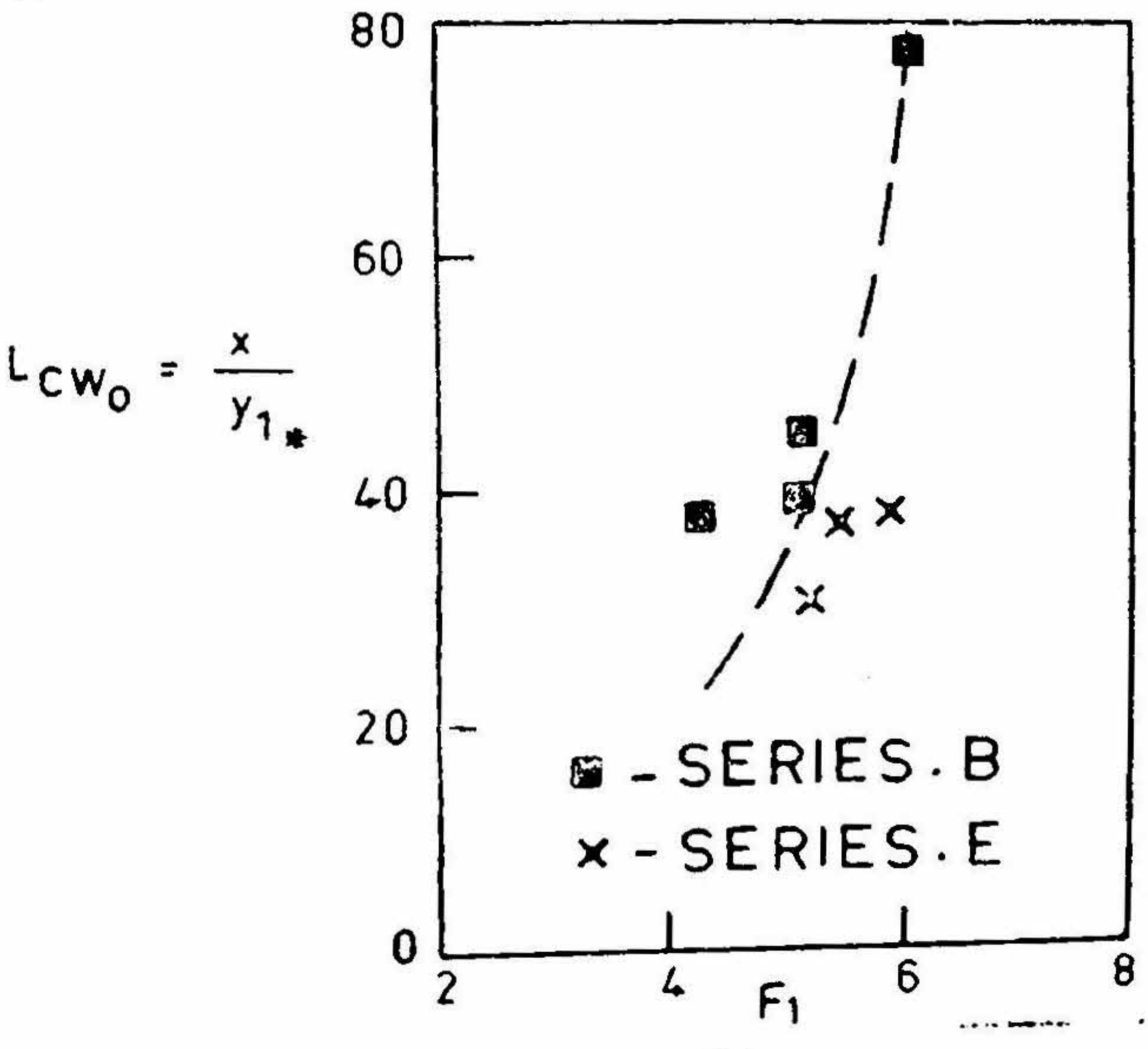

FIG. 15. Variation of L_{cw_o} with Froude number (PHJ).

Conclusions

Although the scatter of points is large in many plots which is understandable in a complex and random phenomenon like the jump as a result of which experimentation becomes difficult, an effort is made here to draw meaningful conclusions based on the trends seen in the several correlation studies.

1. Experimental values exhibit nearly 25% higher sequent depth ratio than those given by Bélanger's equation. In the case of the PHJ this extra value is about 29·5%.

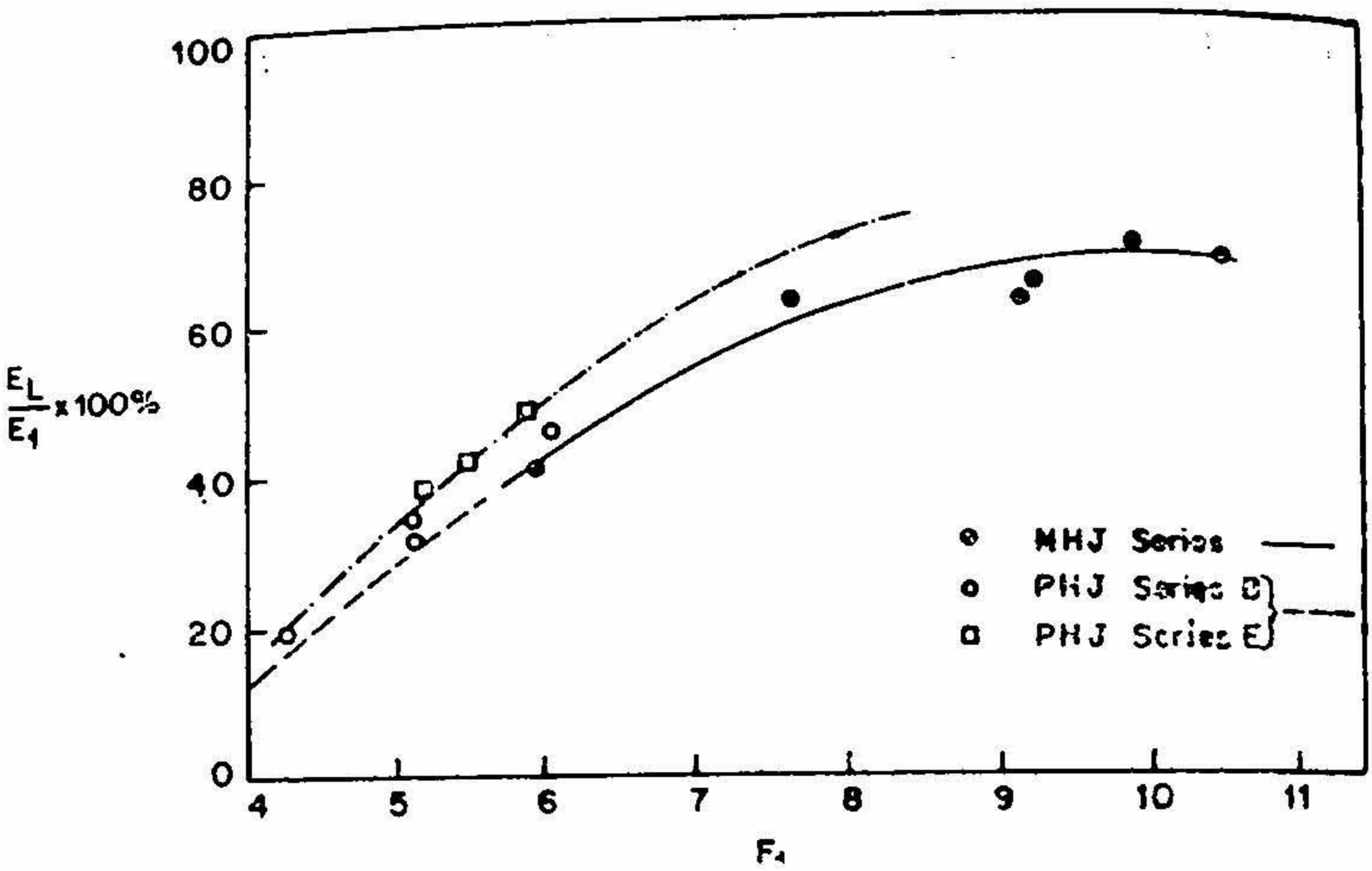

FIG. 16. Correlation of relative energy loss with Froude number.

2. A semitheoretical equation for the sequent depth ratio is presented in the case of the PHJ, taking the upper region of the approaching uniformly serated flow also into account. The sequent depth ratio is influenced by the approaching flow concentration and the major contributing factor is the lower region.

3. The depth at the end of the roller may exceed the sequent depth depending on the Froude number.

4. The length of the jump is arbitrary and may be chosen depending on the requirements. It is found that $L_{cj} > L_{oj} > L_{rj} > L_{ckj} > L_j$. The order of magnitude of L_{rj} and L_R are the same in the case of the NHJ. In the PHJ the length of releasing zone is greater than in the NHJ.

5. The relative energy loss is higher in the PHJ than the NHJ. This difference increases with the Froude number.

References

1. BÉLANGER, J. B. *Essai sur la salution numerique de quelques problems relatifs au mouvement permanent des eaux courantes*, 1828, Carilian Goeury, Paris.

2. HARLEMAN, D. R. F. Discussion on paper—Turbulence characteristics of the hydraulic jump by Rouse *et al.* *Transactions ASCE*, 1959, **124**, 926–966.

3. Advances in Hydrosciences *Hydraulic jump* by Rajaratnam, N., ed. by Chow, V. T., Academic Press. New York and London, 1967, 4. 197–280.

4. RAJARATNAM, N. — The hydraulic jump as a wall jet. *Jl. of Hyd. Dn., Proc. ASCE*, 1965, **91** (Hy. 5), 107–132.

5. LEUTHEUSSER, H. J. AND VISWANATHAN. C. KARTHA — Effects of inflow condition on hydraulic jump. *Jl. of Hyd. Dn., Proc. ASCE*, 1972, **98**, (Hy. 8), 1367–1386.

6. ROUSE, H., SIAO, T. T. AND NAGARATNAM, S. — Turbulence characteristics of the hydraulic jump. *Transactions, ASCE*, 1959, **124**, 926–966.

7. CHOW, V. T. — *Open Channel Hydraulics*, McGraw-Hill Book Co., Inc., New York, 1959.

8. ELEVATORSKII, E. A. — *Hydraulic Energy Dissipators*, McGraw-Hill Book Co., Inc., New York, 1959.

9. SADASIVAN, S. — *Characteristics of a Random Pressure Field on the Boundary of a Free Surface Flow.* A thesis submitted to Department of Civil Engineering in partial fulfilment of Master of Technology Degree of Indian Institute of Technology, Madras, India, 1971.

10. CHANDRASEKHARA SWAMY, N. V. — *Length of the Hydraulic Jump*, Annual Report, Department of Power Engineering, Civil and Hydraulic Engineering Section, Indian Institute of Science, Bangalore, 1959, Pub. No. 13, pp. R5–1 to R5–9.

11. BEHERA, B. AND QURESHY, A. A. — *Length Criterion for the Hydraulic Jump*, Unpublished M.S. Thesis, State University of Iowa, June 1947.

12. MEHROTRA, S. C. — Length of hydraulic jump, *Jl. of Hyd. Dn., Proc. ASCE*, July 1976, 102, Hy. No. 7, p. 12272, pp. 1027–1033.

13. THANDAVESWARA, B. S. — *Self-aerated Flow Characteristics in Developing Zones and in Hydraulic Jumps.* A Ph.D. thesis of the Department of Civil Engineering, Indian Institute of Science, Bangalore, India, July 1974.

14. STRAUB, L. G. AND ANDERSON, A. G. — Experiments in self-aerated flows in open channels. *Jl. of Hyd. Dn., ASCE*, December 1958, **84**, Hy. 7, p. 1890, pp. 1890–1 to 1890–34.

15. LAKSHMANA RAO, N. S. AND GANGA-DHARIAIH, T. — Self-aerated flow characteristics in wall region, *Jl. of Hyd. Dn., Proc. ASCE*, 1971, **97**, Hy. 9, 1285–1303.

16. LAKSHMANA RAO, N. S., SEETHARAMIAH, K. AND GANGA-DHARAIAH, T. — Characteristics of self-aerated flows. *Jl. of Hyd. Dn., Proc. ASCE*, 1970, **96**, Hy. No. 2, p. 7055, 331–355.

17. EHRENBERGER, R. — Wasserbewegung in steilen rinnen (schusstennon) mit besonderberuksichtigung der selbstbelüftung. *Zeitsctorift des Oesterreichischer Ingenieur und Architekten—Verens*, 1926, Nos. 15, 16, 17, 18.

18. SIGALLA, A. — Measurement of skin friction in a plane turbulent wall jet. *Jl. of Roy. Aero. Soc.*, 1958, **62**, 873–877.

19. LAKSHMANA RAO, N. S. and THANDAVESWARA, B. S. The characteristics of aerated free surface flows—present status, *Proc. of the Symp. on Modern Trends in Civil Engineering*, Department of Civil Engineering, University of Roorkee, U.P., India, 1972, November 11-13, 82–88.

20. RAJARATNAM, N. *Some Studies on the Hydraulic Jump*, A Ph.D. thesis of the Department of Power Engineering, Indian Institute of Science, Bangalore, India, 1961.

Appendix I

b Mixing width;

C Air concentration;

E_L Energy loss;

E_1 Specific energy at section 1–1;

F_1 Initial Froude number with respect to initial depth of flow (PHJ); $\bar{V}_1/\sqrt{gy_{1*}}$;

F_4 Initial Froude number with respect to initial depth of flow (NHJ); $\bar{V}_1/\sqrt{gy_1}$;

L Different definitions of the length of the jump;

p_f Integrated shear force;

Q Discharge in lits/sec.;

Re_1 Reynolds number with respect to mean depth;

v Local velocity;

$\bar{V}$ Mean velocity;

x Longitudinal distance along the jump from toe;

y Local depth;

y_1, y_{1*} Initial depth of flow for the NHJ and the PHJ;

y_2, y_{2*} Sequent depths of NHJ and PHJ;

y_r Depth at the roller end;

δ Wall turbulent thickness;

ν Kinematic viscosity;

τ_0 Wall shear;

ϕ Sequent depth ratio;

NHJ Normal hydraulic jump;

PHJ Pre-entrained hydraulic jump.